Journal of Chromatography A, 1218 (2011) 258–262

Contents lists available at ScienceDirect

Journal of Chromatography A

journal homepage: www.elsevier.com/locate/chroma

Nucleic acid affinity of clustered-charge anion exchange adsorbents: Effects of ionic strength and ligand density

Wen-hsiang Chen[a], Joseph Y. Fu[a], Katerina Kourentzi[a], Richard C. Willson[a,b,*]

[a] Department of Chemical Engineering, University of Houston, 4800 Calhoun, Houston, TX 77204-4004, USA
[b] Department of Biology and Biochemistry, University of Houston, 4800 Calhoun, Houston, TX 77204-5001, USA

ARTICLE INFO

Article history:
Received 15 September 2010
Received in revised form 8 November 2010
Accepted 11 November 2010
Available online 18 November 2010

Keywords:
Ion-exchange chromatography
Clustered charge
Nucleic acids
Adsorption
Ligand density

ABSTRACT

In previous work we demonstrated the improved protein-binding capacity and selectivity of ion-exchange adsorbents displaying a "clustered" rather than random, distribution of surface charges. For example, anion-exchange adsorbents displaying 5 mM of positive charge in the form of 1 mM penta-argininamide show much higher affinity and capacity for alpha-lactalbumin than do adsorbents displaying the same 5 mM total charge in the form of single dispersed argininamide charges. We also found that clustered adsorbents selectively favor proteins with inherent charge clustering. In the present work, "clustered" penta-argininamide adsorbents showed DNA binding capacity comparable to that of conventional dispersed adsorbents with 10–100-fold higher ligand density. We also observed that at moderate ionic strength the DNA affinity of all adsorbents tested *increased* with salt while RNA affinity decreased, so that selectivity for DNA over RNA was enhanced as salt concentration increased.

1. Introduction

Ion-exchange chromatography is widely used for the separation of biomolecules [1,2] due to the strength and reversibility of ion-exchange adsorption, and the possibility of tuning selectivity and resolution for the biomolecule of interest [3–7]. The recent increased need for nucleic acids in biological sciences and in medicine (e.g., for plasmid DNA vaccines [8–12]), has called for improved techniques for nucleic acid purification. Thus, there is an on-going interest in improving the affinity and selectivity of ion-exchange adsorbents for nucleic acids.

Traditional ion-exchange adsorbents display a random charge distribution which creates a heterogeneous landscape of adsorption sites [13] and fortuitous charge clustering and geometric matching between adsorbates and adsorbent play an important role in adsorption. For the ion-exchange capture of small ions, a distance-of-charge-separation approach showed that the close proximity of the positive charges on the nitrogen atoms of a polyamine ligand improved its selectivity for divalent (SO_4^{2-}) over monovalent (Cl^-, NO_3^-) ions compared to isolated distributed tertiary and quaternary amine functionalities [13–16]. In our previous work, a higher affinity and capacity for negatively charged proteins was observed for an adsorbent displaying uniform-size clusters of positive charges, than for an adsorbent with the same total charge density displayed as dispersed charges [7]. It was also shown that proteins with highly charged patches were particularly favored in both binding capacity and selectivity on the clustered-charge adsorbent.

In the present work, we tested the capacity and selectivity of clustered-charge anion exchangers for nucleic acids, which display high charge densities compatible with multivalent interactions with clustered adsorbents. It was shown that clustered-charge adsorbents of relatively low ligand density can have a higher DNA affinity than the conventional adsorbents of much higher ligand density. Clustered charge adsorbents also showed enhanced selectivity for DNA over RNA, which can be useful for practical purposes.

2. Experimental

2.1. Materials

AminoLink coupling resin, AminoLink reductant and Micro BCA protein assay kits were from Pierce (Rockford, IL). Q Sepharose Fast Flow and DEAE Sepharose were from GE Healthcare (Piscataway, NJ). Penta-argininamide was custom synthesized by Biomatik (Wilmington, DE); the amide was introduced to avoid the formation of a zwitterionic adsorbent ligand also displaying a negatively charged C-terminal carboxylate. Salmon sperm DNA was from Stratagene (La Jolla, CA). DEAE Plasmid *Plus* resin was from Qiagen (Valencia, CA). Baker's yeast RNA and all other reagents were from Sigma Aldrich (St. Louis, MO).

* Corresponding author at: University of Houston, Department of Chemical Engineering, 4800 Calhoun Avenue, Houston, TX 77204-4004, USA.
Tel.: +1 713 743 4308; fax: +1 713 743 4323.
E-mail address: willson@uh.edu (R.C. Willson).

0021-9673/$ – see front matter © 2010 Elsevier B.V. All rights reserved.
doi:10.1016/j.chroma.2010.11.024

2.2. Adsorbent preparation

Four mL of well-suspended AminoLink coupling resin was placed in a 10 mL disposable polypropylene filter column from Pierce (Cat no 29924) and washed with 10 mL of coupling buffer (0.1 M sodium phosphate buffer, 0.15 M NaCl, pH 7.2) to remove preservatives, then mixed with 2 mL of penta-argininamide solution (3, 6, 12 or 30 mM) on a Cole-Parmer Roto-torque gyratory rotator at room temperature for at least 4 h, and then at 4 °C for 4 days. The supernatant was then drained, and the adsorbent washed with 10 mL of coupling buffer to remove unbound peptide. The adsorbent was then mixed with 2 mL of 66 mM sodium borohydride in 25% ethanol/75% PBS, followed by 30 min rotation to deactivate any remaining aldehyde groups, and washed with 15 mL of 1 M NaCl and 5 mL of storage buffer (10 mM Tris–HCl, pH 8.0), drained and resuspended in 0.67 adsorbent volume of binding buffer (10 mM Tris–HCl, 10 mM NaCl, pH 8.0).

The concentration of peptide ligand on the adsorbent was determined by bicinchoninic acid assay (Micro BCA Protein Assay, Pierce) of the residual supernatant peptide and the modified adsorbent itself. Peptide adsorbents with a final ligand density of 1.4, 2.4, 4.8 and 24 mM penta-argininamide were prepared and stored at 4 °C for later use.

Q Sepharose Fast Flow, Qiagen DEAE Plasmid Plus resin and GE Healthcare DEAE Sepharose were vortexed and placed in a 10 mL disposable polypropylene filter column from Pierce (Rockford, IL). Each adsorbent (4 mL slurry as supplied by the manufacturer) was washed with 10 mL of binding buffer (10 mM Tris–HCl, 10 mM NaCl, pH 8.0) to remove preservatives, drained and then resuspended by adding 0.67 packed adsorbent volume of binding buffer. The ligand density of Qiagen DEAE Plasmid Plus resin was determined to be 125 ± 5 mM by titrating the resin with 5.5 M NaOH using a Metrohm Titrino model 794 titrator, while those of GE Healthcare DEAE and Q Sepharose Fast Flow were supplied by the manufacturer.

2.3. Adsorption isotherm measurement

Each adsorbent (25 μl suspension; 15 μl settled adsorbent volume) was aliquoted into 1.5 mL Eppendorf tubes and incubated with different volumes of nucleic acid stock solution (10–320 μl of 25 μg/mL DNA stock solution in binding buffer or 20 μg/mL RNA stock solution in binding buffer) plus binding buffer to bring the total volume to 1.0 mL plus 15 μl of settled adsorbent. Adsorption was then allowed to equilibrate on a gyratory rotator at room temperature for 1 h, a time found in control experiments to be sufficient for equilibration. After a 10-min centrifugation at 16,000 × *g* in an Eppendorf model 5415D microcentrifuge, the nucleic acid concentration in the supernatant was quantified by 260 nm absorbance using a Beckman-Coulter DU 530 spectrophotometer. The adsorbent pellets were resuspended in 1 mL of binding buffer and again centrifuged (this supernatant contained a negligible quantity of nucleic acid); bound nucleic acids were eluted with 1 mL of elution buffer (binding buffer + 1 M NaCl) and analyzed spectrophotometrically for determination of bound nucleic acid content and calculation of total mass recovery.

2.4. Data analysis

The mass balances (nucleic acid remaining in supernatant + nucleic acid eluted from adsorbent, divided by nucleic acid originally added) for all adsorption data closed in the range of 83–109%. Adsorption isotherms were fit to the Langmuir isotherm (Eq. (1)) using Igor Pro (WaveMetrics, Lake Oswego, OR; version 6.05) which uses the Levenberg–Marquardt algorithm to search for parameters which minimize χ^2 values, as described previously [7].

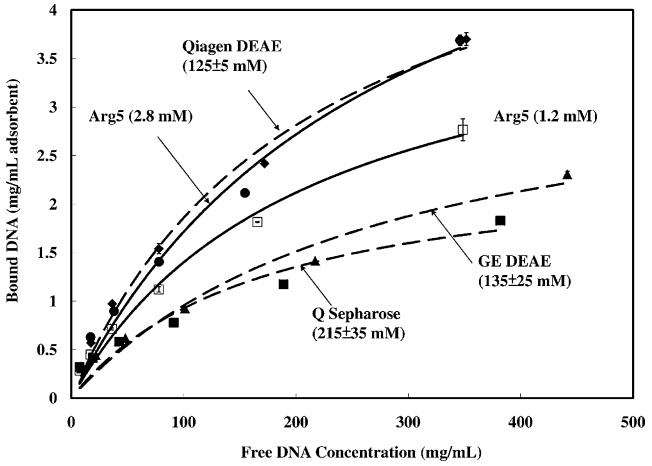

Fig. 1. Adsorption isotherms of salmon sperm DNA with Langmuir fits on Qiagen DEAE resin (♦), GE DEAE Sepharose (▲), penta-argininamide adsorbents (Arg_5: 1.2 mM ligand density (□); 2.8 mM ligand density (●)), and Q Sepharose (■) at 25 °C in 10 mM Tris, 10 mM NaCl at pH 8.0. Error bars correspond to mean ± 1 SD.

$$y = \frac{Q_{max} \times X}{K_d + X} \quad (1)$$

where *y* is the bound nucleic acid concentration, *X* is the free nucleic acid concentration, Q_{max} is the maximum binding capacity, and K_d is the dissociation constant.

3. Results and discussion

3.1. Adsorption isotherms

The performance of the penta-argininamide adsorbent was compared to conventional adsorbents. As shown in Fig. 1, 1.2 mM penta-argininamide adsorbent gave a higher DNA binding capacity (Q_{max} = 4.4 ± 0.5 mg/mL adsorbent) and stronger initial binding affinity (Q_{max}/K_d = 20.6 mL/mL adsorbent) than both Q Sepharose Fast Flow (Q_{max} = 2.5 ± 0.5 mg/mL adsorbent; Q_{max}/K_d = 14.7 mL/mL adsorbent) and GE DEAE Sepharose (Q_{max} = 3.6 ± 0.8 mg/mL adsorbent; Q_{max}/K_d = 13.0 mL/mL adsorbent). The binding capacity (Q_{max} = 6.6 ± 1.2 mg/mL adsorbent) and initial binding affinity (Q_{max}/K_d = 23.2 mL/mL adsorbent) of an increased-ligand-density penta-argininamide (2.8 mM) adsorbent also compared well to those of Qiagen DEAE resin (Q_{max} = 5.8 ± 0.6 mg/mL adsorbent; Q_{max}/K_d = 27.4 mL/mL adsorbent; Table 1). As shown in Fig. 2, extremely strong RNA initial binding affinity and binding capacity were observed on Q Sepharose Fast Flow adsorbent while the 1.2 mM penta-argininamide and the other two conventional adsorbents (Qiagen DEAE resin and GE DEAE Sepharose) exhibited lower RNA binding capacity (Table 1). It is worth noting that the salt-induced reversibility of the nucleic acids' binding to the penta-argininamide adsorbents underscores the contribution of electrostatic interactions [7] compared to possible formation of hydrogen bonds. While arginine is known to form specific hydrogen bonds via its guanidine group with nucleic acids (e.g., HIV 1 TAR hairpins or supercoiled plasmid DNA) displaying characteristic structural motifs [17–24], this mechanism is less favored with the linear nucleic acids used in the present study.

3.2. Salt and ligand density effects of DNA binding

The effect of salt concentration on nucleic acid binding was investigated with single-point adsorption measurements with an initial DNA loading of 40 μg/mL in the solution on the penta-

Table 1
Values of Langmuir Isotherm Parameters Q_{max} and K_d for adsorption of DNA and RNA on Qiagen DEAE resin, GE DEAE Sepharose, penta-argininamide adsorbents (Arg_5; 1.2 mM or 2.8 mM ligand density), and Q Sepharose at 25 °C in 10 mM Tris, 10 mM NaCl at pH 8.0.

Adsorbent	DNA			RNA			$(Q_{max}/K_d)_{DNA}/(Q_{max}/K_d)_{RNA}$
	Q_{max} (mg/mL adsorbent)	K_d (μg/mL)	Q_{max}/K_d (mL/mL adsorbent)	Q_{max} (mg/mL adsorbent)	K_d (μg/mL)	Q_{max}/K_d (mL/mL adsorbent)	
Qiagen DEAE	5.8 ± 0.6	211 ± 43	27.4	1.6 ± 0.2	109 ± 27	14.3	1.91
GE DEAE Sepharose	3.6 ± 0.8	280 ± 115	13.0	2.8 ± 0.7	192 ± 92	14.4	0.92
Arg_5 (1.2 mM)	4.4 ± 0.5	211 ± 47	20.6	2.1 ± 0.1	5.3 ± 0.1	395	0.051
Arg_5 (2.8 mM)	6.6 ± 1.2	282 ± 88	23.2	–	–	5110[a]	0.0045
Q Sepharose	2.5 ± 0.5	171 ± 79	14.7	148,000 ± 91,000	76,800 ± 43,700	1920	0.0076

[a] Estimated from the data in Fig. 4; free RNA = 0.12 μg/mL and bound RNA = 613 μg/mL adsorbent at 10 mM NaCl; the ratio of bound RNA to free RNA was considered as Q_{max}/K_d.

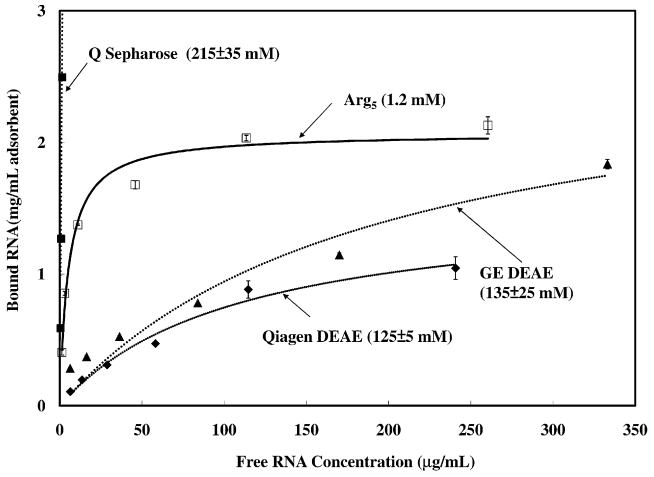

Fig. 2. Adsorption isotherms of Baker's yeast RNA with Langmuir fits on Qiagen DEAE resin (♦), GE DEAE Sepharose (▲), penta-argininamide adsorbent (Arg_5; □) and Q Sepharose (■) at 25 °C in 10 mM Tris, 10 mM NaCl at pH 8.0. Error bars correspond to mean ± 1 SD.

argininamide adsorbent with four different ligand densities (Fig. 3) and 12.5 μg/mL on the penta-argininamide adsorbents and the three conventional adsorbents (Fig. 4). We observed that the binding affinity of DNA for all the adsorbents increased with increasing salt concentration, and then decreased rapidly when the salt concentration reached a specific but different point for each adsorbent (Figs. 3 and 4). We believe that the initial increase of DNA binding affinity with increasing salt concentration is due to counterion shielding of intermolecular repulsion between anionic DNA molecules as further discussed in Section 3.3.

As shown in Fig. 3 and Table 2, the initial slope of the increase of loading as a function of salt concentration decreased from 4.8 g/L M (at 1.4 mM ligand) to 0.054 g/L M (at 24 mM ligand). As ligand density increased from 1.4 to 4.8 mM penta-argininamide, the maximum DNA binding capacity also increased and the adsorption maximum was observed at higher salt concentration. Complete DNA elution from the 1.4, 2.4 and 4.8 mM penta-argininamide adsorbents was achieved with 1 M NaCl, but the 24 mM penta-argininamide adsorbent required 3 M NaCl. For each ligand density there is a 'critical' salt concentration, above which the adsorbent with higher density binds more DNA; the amount of DNA captured decreases systematically with increasing ligand density as ionic strength increases.

These observations are consistent with stronger kinetic trapping of the DNA at higher ligand densities and lower ionic strength, impairing DNA access to buried, inaccessible ligands. At the loading maximum, assuming that DNA evenly penetrates only 5% of the radius of the adsorbent volume (the precise number is not essential to the arguments which follow; particles are assumed to consist of spherical particles of 105 μm mean diameter) [8], the inter-DNA

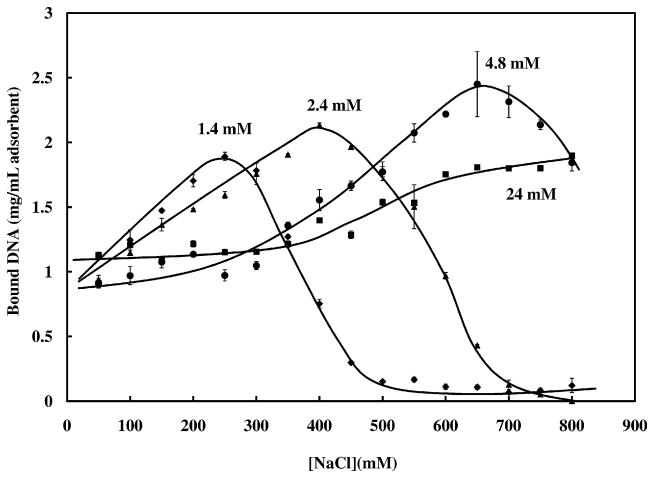

Fig. 3. Single point adsorption measurements of salmon sperm DNA as a function of salt concentration on penta-argininamide (Arg_5) adsorbents with varying ligand densities: 1.4 mM (♦), 2.4 mM (▲), 4.8 mM (●) and 24 mM (■) at 25 °C in 10 mM Tris, pH 8.0 as a function of salt concentration. The initially offered loading of DNA was 40 μg/mL buffer (2.67 mg/mL adsorbent). Note that the curves are generated by connecting the data points for each adsorbent and error bars correspond to mean ± 1 SD.

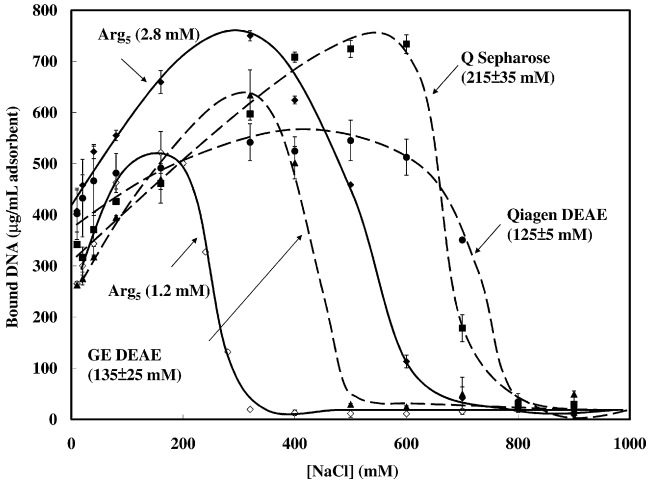

Fig. 4. Single point DNA adsorption measurements as a function of salt on Qiagen DEAE resin (●), GE DEAE Sepharose (▲), penta-argininamide adsorbents (Arg_5: 1.2 mM ligand (◊); 2.8 mM ligand (♦)), and Q Sepharose (■) at 25 °C in 10 mM Tris at pH 8.0 at varying added NaCl concentrations. The initial loading of DNA was 12.5 μg/mL buffer (830 μg/mL adsorbent). Note that the curves are generated by connecting the data points for each adsorbent and error bars correspond to mean ± 1 SD.

Table 2
Inter-adsorbate distance and charge ratio of adsorbate to adsorbent at the maxima in Fig. 6.

Adsorbent	Interligand distance (Å)	Ligand charge density (mM)	DNA maximum capacity (mg/mL)	DNA charge density (mM)	Inter-DNA distance (Å)	Charge ratio of DNA/ligand	Initial Slope (g/LM)	Slope after maxima (g/LM)
Arg_5 (1.4 mM)	106	7	1.89	5.72	61.8	0.82	4.8	−10.0
Arg_5 (2.4 mM)	88	12	2.13	6.45	58.2	0.54	3.2	−5.6
Arg_5 (4.8 mM)	70	24	2.45	7.42	54.2	0.31	1.8	−4.0

Note: interligand distance is 41 Å and initial slope is 0.054 g/LM for Arg_5 (24 mM).

distance (estimated as the inverse cube root of the volume occupied per DNA molecule) decreases from 464 to 426 Å, and the ratio of total charge of bound DNA to the ligand in the outer 5% of the adsorbent ranges from 5.5 (at 1.4 mM ligand) to 2.1 (at 4.8 mM ligand). If DNA only adsorbs on the surface of the adsorbent particles, the two-dimensional inter-DNA distance decreases from 61.8 to 54.2 Å.

Increasing ligand density does not result in a proportional increase in DNA loading and the charge ratio of total bound DNA to the ligand at the loading maximum; this may be due to pore accessibility limitations and steric hindrance by already adsorbed DNA macromolecules [25,26]. Although DNA is known not to penetrate well into ion-exchange adsorbents (the pore size of the agarose adsorbent used in our work is about 30 nm [27] which equals to 2/3 of the estimated DNA persistence length), a kinetic trapping mechanism requires at least partial penetration of DNA into the adsorbent, or all ligand densities would produce identical results. The limiting case of adsorption is one molecule of DNA per molecule of ligand, corresponding to roughly 2300 negative charges of DNA (of average size 1150 bp) being captured by the penta-argininamide ligand with 5 positive charges. Assuming uniform distribution of the ligand throughout the adsorbent volume, and that DNA molecules adsorb solely on the surface of the adsorbent particles, all ligands within a distance of 50-fold the Debye length would be required to provide at least one ligand per DNA molecule for the 250 mM NaCl maximum adsorption of DNA on the 1.4 mM penta-argininamide adsorbent (the Debye ionic shielding length for an aqueous solution of NaCl, a 1:1 electrolyte, is estimated as: Debye length, k^{-1} (Å) = $3 \times (I^{-0.5})$, where I is the ionic strength in M [28]). Since counterion shielding would be complete at a much shorter distance, some degree of penetration into the adsorbent must occur, consistent with kinetic trapping.

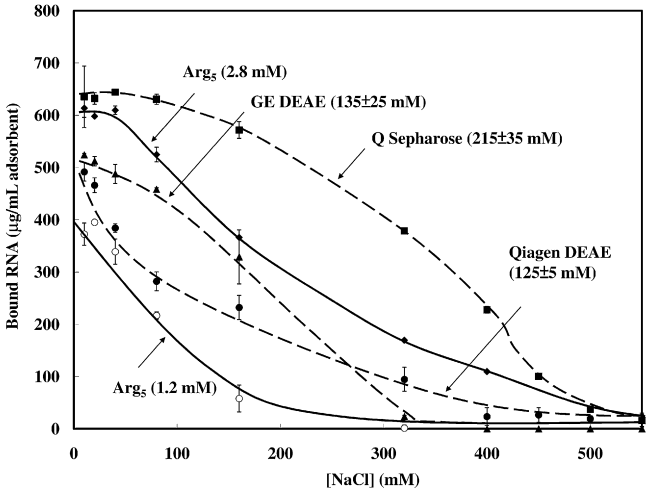

Fig. 5. Single point RNA adsorption measurements on Qiagen DEAE resin (●), GE DEAE Sepharose (▲), penta-argininamide adsorbents (Arg_5: 1.2 mM ligand (○); 2.8 mM ligand (♦)) and Q Sepharose (■) at 25 °C in 10 mM Tris at pH 8 at varying added NaCl concentrations. The initial loading of RNA was 10 μg/mL buffer (670 μg/mL adsorbent). Note that the curves are generated by connecting the data points for each adsorbent and error bars correspond to mean ± 1 SD.

3.3. Salt effects of RNA binding and the selectivity for DNA/RNA

The effect of salt concentration on RNA was investigated with initial loading of RNA of 10.0 μg/mL, and we further compared the salt effect between DNA and RNA. A decreasing fraction of offered RNA bound with increasing salt concentration (Fig. 5) while the DNA/RNA binding capacity ratio of the 1.2 mM penta-argininamide adsorbent increased 9-fold when NaCl concentration was increased from 10 to 160 mM (Fig. 6).

As discussed above the counterion shielding may play an important role in these effects. The Debye length is 30 Å at 10 mM and 6.0 Å at 250 mM, while the contour and persistence lengths of a 1000-bp DNA fragment are 570 Å and 450 Å [29,30], respectively (Table 3). This implies that DNA molecules will be both "stiff" and mutually electrostatically repulsive at low salt concentration. As the salt concentration increases, the Debye length decreases and repulsion is shorter-ranged, although the stiffness of DNA does not change as rapidly. The average center-to-center spacing of penta-argininamide charged ligands at 2.4 mM concentration, assumed to be uniformly distributed throughout the adsorbent volume, is 88 Å (Table 2) while the comparable ligand spacings are 24 Å, 19 Å and 23 Å for Qiagen DEAE resin, Q Sepharose and GE DEAE Sepharose, respectively. Each of these is substantially smaller than the persistence length of DNA (but not RNA) under the conditions used. As a result, increased ionic strength reduces intermolecular repulsion between the stiff DNA molecules, and thus effective DNA loadings are increased. Further increases in ionic strength suppress adsorption by the classic counterion mass-action ion-exchange elution mechanism [25,26]. RNA is over 20-fold more flexible than DNA;

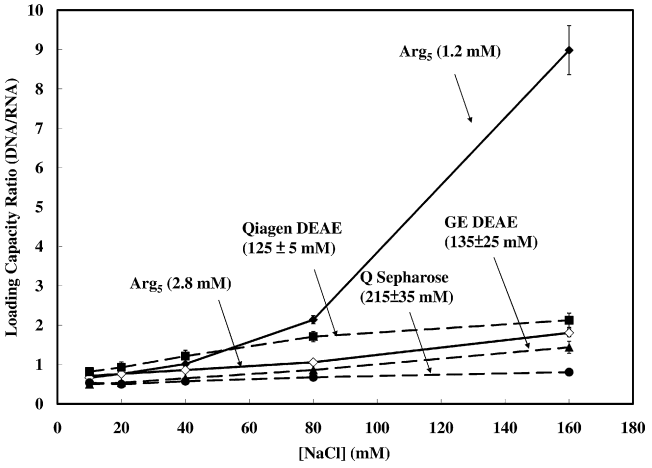

Fig. 6. Comparison of loading capacity ratio (the ratio of bound DNA to bound RNA) among Qiagen DEAE resin (●), GE DEAE Sepharose (▲), penta-argininamide adsorbents (Arg_5: 1.2 mM ligand (♦); 2.8 mM ligand (◊)) and Q Sepharose (■) at 25 °C in 10 mM Tris at pH 8.0 at varying salt concentrations. The initial loadings of DNA and RNA were 12.5 μg/mL and 10.0 μg/mL, respectively. Error bars correspond to mean ± 1 SD.

Table 3
Comparison of persistence length and Debye length values for DNA and RNA at different salt concentrations.

	[NaCl] (mM)	Debye length (Å)	Intrinsic persistence[a] length l_p^0 (Å)	Persistence length[a] ($l_p = l_p^0 + l_p^e$) (Å)
DNA (300–1000 bp)	5	42.4	450	806
	10	30.0	450	570
	150	7.74	450	450
	250	6.0	450	450
	350	5.1	450	450
	700	3.6	450	450
RNA[b] (190 bases)	10	30.0	10	21
	250	6.0	10	10

[a] Note that for most of the DNA species, the non-electrostatic contribution to DNA stiffness in monovalent salt is taken to be 450 Å as the intrinsic (non-electrostatic) persistence length [25–27]; for a 190-base RNA, the intrinsic persistence length is 10 Å [27].
[b] Data for RNA were from Ref. [30].

the persistence length of a 190-base RNA fragment is only 21 Å at 10 mM NaCl and 10 Å at 250 mM NaCl. The flexibility of RNA minimizes intermolecular electrostatic repulsion by mutual avoidance (and possibly also allows RNA molecules to assume a configuration optimized to interact with as many adsorbent charges as possible), so that even when the Debye length and intermolecular repulsion decreases (as salt increases), the binding of RNA to the adsorbent is not enhanced.

4. Conclusions

The current work establishes the utility of clustered-charge ion-exchange adsorbents in the capture of nucleic acids. When compared to conventional adsorbents, penta-argininamide clustered adsorbents showed stronger selectivity for DNA vs. RNA binding by adjusting the salt concentration. The current studies also suggested that uniform clustered ligands possess multiple homogeneous binding sites that enhance the multivalent binding of the adsorbates, in a similar manner as that in which Jennissen and Demiroglou [31] optimized protein purification with critical hydrophobic interaction chromatography (HIC) using different immobilized alkyl ligand concentrations. This further suggests the possibility of optimization of other modes, e.g., IMAC separations using metal-chelating ligand clusters rather than traditional IMAC ligands.

Acknowledgements

This research was funded by grants from NSF (grant CTS-0004544) and the Robert A. Welch Foundation (grant E-1264). We would like to thank Indhu Kanakaraj and Mohan Vivek for helpful discussions.

References

[1] H.C. Thomas, J. Am. Chem. Soc. 66 (1944) 1664.
[2] N.K. Boardman, S.M. Partridge, Biochem. J. 59 (1955) 543.
[3] D.J. Roush, D.S. Gill, R.C. Willson, J. Chromatogr. A 653 (1993) 207.
[4] D.S. Gill, D.J. Roush, R.C. Willson, J. Chromatogr. A 684 (1994) 55.
[5] D.S. Gill, D.J. Roush, R.C. Willson, J. Colloid Interface Sci. 167 (1994) 1.
[6] D.S. Gill, D.J. Roush, K.A. Shick, R.C. Willson, J. Chromatogr. A 715 (1995) 81.
[7] J.Y. Fu, S. Balan, A. Potty, V. Nguyen, R.C. Willson, Anal. Chem. 79 (2007) 9060.
[8] A. Ljunglof, P. Bergvall, R. Bhikhabhai, R. Hjorth, J. Chromatogr. A 844 (1999) 129.
[9] J.C. Murphy, J.A. Wibbenmeyer, G.E. Fox, R.C. Willson, Nat. Biotechnol. 17 (1999) 822.
[10] S. Balan, J. Murphy, I. Galaev, A. Kumar, G.E. Fox, B. Mattiasson, R.C. Willson, Biotechnol. Lett. 25 (2003) 1111.
[11] J.C. Murphy, G.E. Fox, R.C. Willson, J. Chromatogr. A 984 (2003) 215.
[12] J.C. Murphy, D.L. Jewell, K.I. White, G.E. Fox, R.C. Willson, Biotechnol. Prog. 19 (2003) 982.
[13] S. Subramonian, D. Clifford, React. Polym. 9 (1988) 195.
[14] D. Clifford, W.J. Weber Jr., React. Polym. Ion Exch. Sorb. 1 (1983) 77.
[15] S. Subramonian, D. Clifford, J. Solution Chem. 18 (1989) 529.
[16] L.L. Horng, D. Clifford, React. Funct. Polym. 35 (1997) 41.
[17] R.Y. Tan, A.D. Frankel, Biochemistry 31 (1992) 10288.
[18] J.D. Puglisi, L. Chen, A.D. Frankel, J.R. Williamson, Proc. Natl. Acad. Sci. U.S.A. 90 (1993) 3680.
[19] K.T. Dayie, A.S. Brodsky, J.R. Williamson, J. Mol. Biol. 317 (2002) 263.
[20] C.F. Landes, Y.N. Zeng, H.W. Liu, K. Musier-Forsyth, P.F. Barbara, J. Am. Chem. Soc. 129 (2007) 10181.
[21] J.S. Tao, A.D. Frankel, Proc. Natl. Acad. Sci. U.S.A. 89 (1992) 2723.
[22] F. Sousa, T. Matos, D.M.F. Prazeres, J.A. Queiroz, Anal. Biochem. 374 (2008) 432.
[23] F. Sousa, D.M.F. Prazeres, J.A. Queiroz, Biomed. Chromatogr. 23 (2009) 160.
[24] F. Sousa, D.M.F. Prazeres, J.A. Queiroz, J. Gene Med. 11 (2009) 79.
[25] C.A. Brooks, S.M. Cramer, AIChE J. 38 (1992) 1969.
[26] J.A. Gerstner, J.A. Bell, S.M. Cramer, Biophys. Chem. 52 (1994) 97.
[27] Y. Yao, K.J. Czymmek, R. Pazhianur, A.M. Lenhoff, Langmuir 22 (2006) 11148.
[28] Z.J. Guo, C.H. Taubes, J.E. Oh, L.J. Maher, U. Mohanty, J. Phys. Chem. B 112 (2008) 16163.
[29] J.B. Hays, M.E. Magar, B.H. Zimm, Biopolymers 8 (1969) 531.
[30] G. Caliskan, C. Hyeon, U. Perez-Salas, R.M. Briber, S.A. Woodson, D. Thirumalai, Phys. Rev. Lett. 95 (2005) 4.
[31] H.P. Jennissen, A. Demiroglou, J. Chromatogr. A 1109 (2006) 197.